https://doi.org/10.5194/egusphere-2026-4763
Preprint. Discussion started: 15 September 2026

Dynamic Cross-Sensor Calibration for Low-Cost Particulate Matter Sensors

Megan A. Mirkhanian[1], Rufus D. Edwards[1], Tracy Allen[2]
[1]Department of Environmental and Occupational Health, Joe C. Wen School of Population and Public Health, University of California, Irvine, Irvine, CA, 92697, USA
[2]Electronically Monitored Ecosystems, LLC, Benicia, CA 94510, USA
Correspondence to: Rufus D. Edwards (edwardsr@hs.uci.edu)

Abstract

Low-cost particulate matter (PM) sensors are increasingly used for air-quality and occupational exposure monitoring, but their mass-concentration response can vary with aerosol size distribution and combustion source. This variation limits measurement accuracy in environments where particle properties change over time and space, including wildfire smoke settings. We developed a real-time dynamic calibration method for a dual-sensor platform combining an Analog Devices ADPD188BI blue-light photometric sensor with a Sensirion SPS30 low-cost optical particle counter to improve $PM_{1.0}$ mass-concentration estimates. Nebulized monodisperse polystyrene latex spheres with diameters of 0.49, 0.60, 0.72, 0.83, and 0.88 µm were measured with a Lasair 1003 optical particle counter to characterize the particle-size-dependent responses of both sensors. The SPS30 $PM_{1.0}$ output and ADPD188BI blue-LED signal exhibited distinct size-dependent responses, providing the basis for adjustment using paired sensor measurements. We developed a ratio-based framework in which the instantaneous ADPD188BI blue-LED-to-SPS30 response ratio was used to estimate a $PM_{1.0}$ mass-conversion coefficient. The method was evaluated against gravimetric $PM_{1.0}$ measurements from separate combustion experiments involving pine and oak under both smoldering and flaming conditions, and bamboo and candles under smoldering conditions only. Both sensor outputs were strongly linearly related to gravimetric $PM_{1.0}$ within individual combustion conditions (SPS30, $R^2 = 0.992$-0.999; ADPD188BI blue-LED, $R^2 = 0.990$-0.998), although regression slopes varied across aerosol sources and conditions. Applying the dynamic adjustment improved agreement with gravimetric $PM_{1.0}$ across the tested combustion aerosols, reducing the pooled root mean square error (RMSE) by 84.5 %. These findings support the use of paired low-cost optical sensors to adjust $PM_{1.0}$ mass response in changing smoke environments. Further evaluation is needed in wearable and field-deployed systems for wildland firefighter exposure monitoring, where routine use of reference instruments is often impractical.

1. Introduction

Low-cost particulate matter (PM) sensors are portable, relatively inexpensive, and capable of providing measurements at high spatial and temporal resolution, with applications including characterizing local ambient PM gradients in urban areas (Penchala et al., 2025), monitoring occupational exposures (Khan et al., 2021), and supporting the interpretation of aerosol optical depth measurements in areas where fixed-site monitors are not present (Ruiter et al., 2023). In occupational settings, this spatial and temporal resolution enables detailed characterization of exposure patterns and can support the implementation of control measures through direct feedback. For example, low-cost PM sensors can be integrated with real-time audio warning systems to help wildland firefighters determine when air-purifying respirators should be worn during high-exposure tasks and to inform task assignments based on cumulative exposure (Edwards et al., 2005). These advantages are limited, however, by uncertainty in sensor accuracy relative to reference instruments and by differences between the particle-size fractions reported by low-cost sensors and those used in regulatory exposure standards (Ruiter et al., 2020). Sensor performance also varies with aerosol properties, workplace conditions, and deployment practices (Ruiter et al., 2020).

Most low-cost PM sensors used for aerosol monitoring rely on light scattering. In photometric sensors, particles are measured as an ensemble and the integrated scattered-light signal is related to PM mass, whereas optical particle counters (OPCs) detect individual particles, assign them to size bins, and estimate mass from the resulting size distribution (Hagan and Kroll, 2020). For both sensor types, reported PM concentrations depend on particle size distribution, refractive index, relative humidity, and the assumptions used to convert optical response to particle mass (Giordano et al., 2021; Hagan and Kroll, 2020). Photometric sensors are affected primarily by variation in the relationship between integrated scattering and particle mass, whereas OPCs are additionally affected by particle-sizing uncertainty and count-to-mass conversion assumptions (Hagan and Kroll, 2020; Kuula et al., 2020). Because scattering also depends on particle diameter relative to the illumination wavelength and on aerosol optical properties, responses can differ between sensors operating at different wavelengths (Hagan and Kroll, 2020).

Despite their advantages, concerns remain regarding the accuracy of low-cost PM sensors relative to reference monitoring instruments (Jayaratne et al., 2020; Molina Rueda et al., 2023; Zou et al., 2021). Some early low-cost particle monitors combined ionization and light-scattering detection to obtain complementary responses across the particle-size distribution (Pillarisetti et al., 2023). Most current low-cost monitors rely primarily on optical sensors because they enable compact, low-power, real-time measurements. However, the relationship between optical response and aerosol mass depends on particle size distribution and aerosol optical properties. Calibration relationships developed for one aerosol may therefore not transfer to other sources, as reported in laboratory (Analog Devices, 2020; Dong et al., 2023; Hinds William and Zhu Yifang, 2022; Reid et al., 2005) and field studies (Giordano et al., 2021; Hagan and Kroll, 2020; Molina Rueda et al., 2023; U.S. Environmental Protection Agency, n.d.; Zou et al., 2021). When a single sensitivity factor is applied to heterogeneous aerosols, PM mass concentrations may be over-

https://doi.org/10.5194/egusphere-2026-4763
Preprint. Discussion started: 15 September 2026

or underestimated because the particle size distribution is unknown and concurrent gravimetric measurements are often unavailable (Giordano et al., 2021; Tryner et al., 2020).

Wildland firefighters are exposed to smoke plumes with particle size distributions that vary rapidly across space and time because of differences in location within the fire environment, fuel type, combustion phase, and plume aging. Here, we present a dynamic calibration framework that combines an OPC and a photometer sampling the same airstream to adjust PM mass concentrations in real time. Sensor responses were characterized using monodisperse polystyrene latex (PSL) spheres and combustion aerosols generated from bamboo, pine, oak, and candles in a controlled aerosol-testing chamber. The framework uses the ratio of the two sensor responses, which exhibit different particle-size-dependent sensitivities, as an indicator of changes in the size distribution of particles ≥ 0.3 µm. This ratio is then used to estimate the mass-response coefficient for an uncharacterized aerosol. Although developed for wildland firefighter exposure monitoring, this approach may also be applicable to other settings involving spatially or temporally heterogeneous aerosols.

2. Materials and Methods

2.1 Particulate Matter Sensors

The particle monitor included an SPS30 (Sensirion; Stäfa, Switzerland) an optical particle counter that uses a 660 nm red laser and a 90° scattering angle, combined with an ADPD188BI optical scattering photometer (Analog Devices, Inc., Wilmington, MA, USA) which uses a 470 nm blue LED and operates with a mean backscatter angle of 85° (±50°) (Murphy et al., 2020; Datasheet SPS30 Particulate Matter Sensor for Air Quality Monitoring and Control). In this paper, we consider only the ADPD188BI blue-LED channel signal and the SPS30 $PM_{1.0}$ measurement; accordingly, ADPD188BI refers to the blue-LED channel, and SPS30 refers to the $PM_{1.0}$ measurement bin throughout.

For wood smoke particles from wildfires mass median diameters commonly range from 0.4 to 0.7 µm but are highly variable depending on combustion conditions (U.S. Department of Agriculture Forest Service, 2016; U.S. Environmental Protection Agency, n.d.). Because Mie scattering intensity differs significantly between 470 nm and 660 nm when particle size is comparable to the optical wavelength, these sensors respond differently to changes in the bulk size distributions of test aerosols ≥ 0.3 µm in diameter. Across six particle-free baseline chamber experiments (6-50 °C), SPS30 mass concentration remained temperature-invariant (slope = 0.0 µg m^{-3} $°C^{-1}$), whereas the ADPD188BI signal exhibited strong temperature dependence (slopes -4 to -14 mA $°C^{-1}$; R^2 = 0.84-0.99), confirming substantial thermal drift in the

https://doi.org/10.5194/egusphere-2026-4763
Preprint. Discussion started: 15 September 2026

photometric signal. To address this drift, a baseline correction was applied to derive a temperature-stable baseline that estimates the temperature-driven dependence of the blue-LED signal using low-quantile smoothing and piecewise interpolation.

2.2 Aerosol-Testing Chamber

All experiments were conducted in a 55 × 55 × 55 cm sealed aerosol-testing chamber (Fig. 1) equipped with an internal circulation fan to promote uniform mixing. The chamber includes an inlet port with a HEPA filter for purging the chamber prior to use and purging between aerosol concentration peaks, and an outlet port located in the fume hood. Aerosol introduction for each run was performed only after the chamber particle count reached $\leq 0.5\ \mu g\ m^{-3}$, as measured by the SPS30. Combustion aerosols were introduced through the inlet by removing the HEPA filter briefly for aerosol entry. After introduction the chamber was then sealed from particles passing through the inlet and outlet ports for ten minutes to maintain the peak concentration, and each source was tested multiple times at different concentrations. A longer averaging window of ten minutes was used because the gravimetric reference reflects particle mass integrated over minutes, whereas second-scale peaks are transient and may not represent the overall source response. Combustion aerosols that were introduced into the chamber included candles and biomass fuels (pine, oak, and bamboo) under either controlled smoldering and or flaming conditions. A second line was used for introducing nebulized monodisperse PSL spheres directly into the chamber.

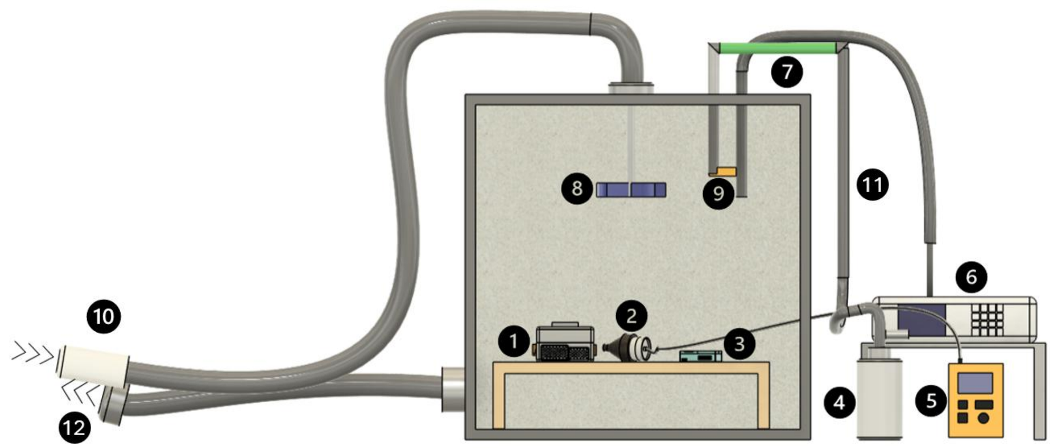

Figure 1. Schematic of the aerosol exposure chamber (shown as square) used for combustion source and polystyrene latex (PSL) sphere experiments. Numbered components indicate the (1) FirefighterPM sensor, including the Analog Devices ADPD188BI and Sensirion SPS30; (2) BGI Triplex cyclone and gravimetric filter cassette assembly; (3) Sensirion SPS30; (4) single-jet Collison nebulizer for PSL sphere aerosol introduction; (5) SKC air sampling pump; (6) Lasair 1003 Optical Particle Counter (OPC); (7) Nafion™ and drying tube; (8) mixing fan; (9) ^{210}Po static eliminator; (10) combustion aerosol inlet; (11) PSL Sphere aerosol path; (12) aerosol exhaust outlet.

2.3 Gravimetric Measurements of Combustion Aerosols

Samples were drawn from the chamber through a BGI Triplex cyclone (model SCC1.062, Mesa Labs, Lakewood, CO, USA). Downstream of the cyclone, particles were collected on a 37 mm PTFE membrane filter (SKC Inc., Eighty Four, PA, USA) mounted in a conductive cassette. A constant-flow using a Universal PCXR8 Pump (SKC) maintained the flow at 3.5 L min^{-1} within ± 2% of the target, verified using a TSI 4140 Mass Flow Meter (TSI Inc., Shoreview, MN, USA) pre- and post- sampling. Filters were conditioned for 24 hours at 20-23 °C (± 2 °C) and 30-40 % relative humidity (± 5 %) prior to weighing, and pre- and post-sampling masses were measured using a Cahn C31 microbalance (Model 10931-01F). Gravimetric $PM_{1.0}$ concentrations were calculated from the net filter mass gain and the time-integrated sample volume (Sect. S1). Gravimetric $PM_{1.0}$ mass concentrations served as a primary reference measurement for comparison with the $PM_{1.0}$ mass concentration size bin of the SPS30 and ADPD188BI blue LED channel. Aerodynamic Particle Sizer (APS) measurements show that the proportion of particles larger than 1 μm in diameter from smoldering and flaming combustion is very low (Dong et al., 2023). Although lower combustion efficiency in moderate fires generally produces larger particles, particle size may also increase in high-intensity fires, indicating that both combustion efficiency and fire intensity influence fresh emission particle size (Reid et al., 2005). Separately, because wildland fire smoke can reach concentrations substantially higher than those typical of ambient particulate pollution, SPS30 performance was evaluated up to the onset of saturation at 3.4 mg m^{-3}, while higher concentrations were evaluated using the ADPD188BI.

2.4 Monodisperse Polystyrene Latex (PSL) Spheres

Monodisperse PSL spheres (0.49, 0.60, 0.72, 0.83 and 0.88 μm diameter; Magsphere Inc., Pasadena, CA, USA) stock solutions were washed via centrifugation to remove residual surfactants and subsequently resuspended in 99.5 % isopropyl alcohol. Detailed PSL sphere preparation steps are provided in the Supporting Information (Sect. S3). The resulting suspensions were aerosolized using a single-jet collision nebulizer (CH Technologies, USA) operated at 20 psi, yielding a stable aerosol flow of 2.0 L min^{-1} ± 2 % verified using a TSI 4140 Mass Flow Meter (TSI). The nebulized aerosol stream passed through a diffusion dryer containing Nafion™ tubing (Perma Pure Inc., Lakewood, NJ, USA; 2.18 mm in ID, 2.74 mm in OD) to reduce humidity prior to entering the chamber. Immediately upstream of the chamber inlet, the PSL spheres were routed through two ^{210}Po static eliminators (NRD LLC, Grand Island, NY, USA) to neutralize electrostatic charge. PSL sphere distributions were characterized using a LASAIR 1003 optical particle counter (Particle Measuring Systems, Boulder, CO, USA) connected to the chamber to assess size ranges after nebulization and drying.

https://doi.org/10.5194/egusphere-2026-4763
Preprint. Discussion started: 15 September 2026

3 Results

3.1 Monodisperse Polystyrene Latex (PSL) Spheres

The SPS30 $PM_{1.0}$ output and ADPD188BI blue-LED signal exhibited distinct size-dependent responses across the 0.49, 0.60, 0.72, 0.83, and 0.88 µm monodisperse PSL spheres (Fig. 2). Figure 2 presents (a) the SPS30 $PM_{1.0}$ mass concentration and (b) the ADPD188BI blue-LED signal across the tested aerosol concentrations, with the Lasair 1003 average particle number concentration at each peak shown on the secondary y-axis. During the PSL experiments, a second SPS30 was used to guide aerosol loading so that each PSL sphere diameter was tested over a comparable chamber concentration range. The observed behavior is consistent with Mie scattering theory, under which optical response depends on particle diameter relative to the incident wavelength. As shown in Fig. 2, the SPS30 $PM_{1.0}$ response and the ADPD188BI blue-LED signal exhibited different size-dependent trends across the 0.49-0.88 µm PSL spheres. Because the ADPD188BI uses a 470 nm blue LED and the SPS30 uses a 660 nm red laser, the two sensors are expected to have different wavelength-dependent sensitivities over this particle size range. The stronger variation in the ADPD188BI signal relative to the SPS30 response demonstrates that the paired sensors provide distinct, complementary optical responses that can be used for dynamic mass-response adjustment.

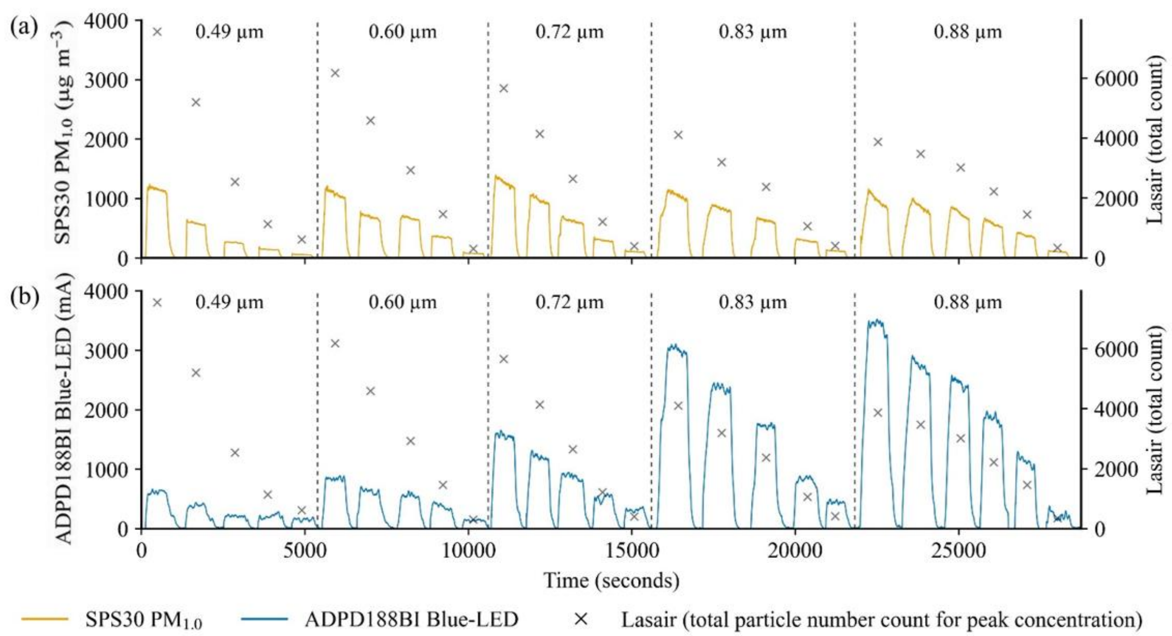

Figure 2. Size-dependent response of the SPS30 and ADPD188BI sensors to monodisperse polystyrene latex (PSL) spheres. Panel (a) shows the SPS30 $PM_{1.0}$ mass concentration, and panel (b) shows the ADPD188BI blue-LED signal for 0.49, 0.60, 0.72, 0.83, and 0.88 µm PSL spheres. The right y-axis indicates the total particle number count measured by the Lasair 1003 optical particle counter, shown as × markers at peak concentrations.

https://doi.org/10.5194/egusphere-2026-4763
Preprint. Discussion started: 15 September 2026

Figure 3 presents the normalized particle number size distributions for the PSL spheres using discrete Lasair 1003 size bins (0.3-0.4, 0.4-0.5, 0.5-0.7, 0.7-1.0, and 1.0-2.0 µm) normalized by the logarithmic width of each size channel to allow comparison across bins of different interval widths. Size intervals were treated as inclusive of the lower bound and exclusive of the upper bound. Panels 3(a-e) show narrow, unimodal peaks that align closely with the manufacturer-reported PSL diameters, confirming that the aerosolized spheres remained well constrained in size after nebulization and drying. This limited polydispersity indicates that the observed differences in sensor response across PSL conditions were primarily driven by changes in particle diameter rather than by broad shifts in size spread or multimodal structure. Additional details on PSL sphere size distributions and the SPS30 number concentration response across PSL sphere diameters are provided in Fig. S1 and Fig. S2.

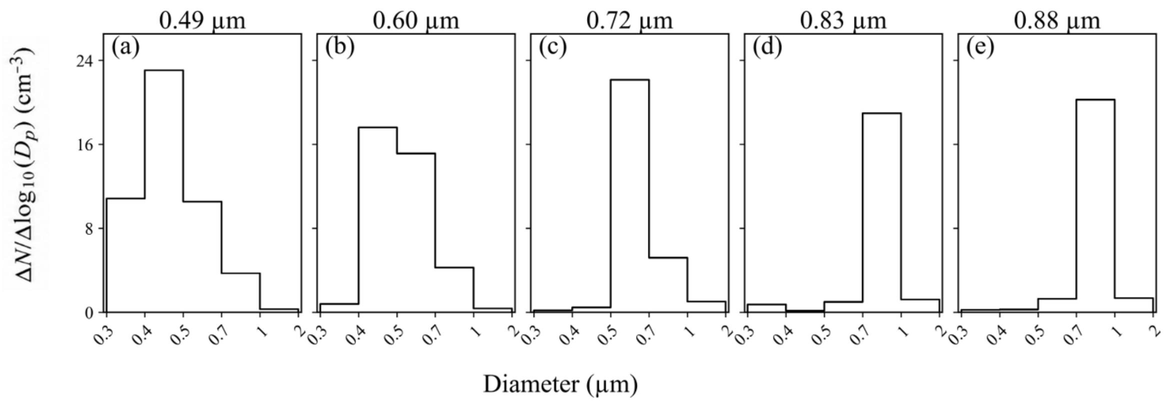

Figure 3. Normalized particle number size distributions for aerosolized polystyrene latex (PSL) spheres. Panels (a-e) show target diameters of 0.49, 0.60, 0.72, 0.83, and 0.88 µm, confirming near-monodisperse aerosols for sensor characterization.

Overall, these results demonstrate that the SPS30 $PM_{1.0}$ and ADPD188BI blue-LED signal have distinct particle-size-dependent responses and can therefore provide complementary size-related information.

3.2 Combustion sources

The SPS30 $PM_{1.0}$ output and ADPD188BI blue-LED signal were strongly linearly related to gravimetric $PM_{1.0}$ within each combustion condition ($R^2 = 0.990$-0.999), although the regression slopes varied among aerosol sources (Fig. 4). Figure 4 presents the responses of (a) the SPS30 $PM_{1.0}$ mass concentration and (b) the ADPD188BI blue-LED channel signal to chamber-generated aerosols from smoldering candle and bamboo combustion and from oak and pine under smoldering and flaming conditions. These differences

https://doi.org/10.5194/egusphere-2026-4763
Preprint. Discussion started: 15 September 2026

207 indicate that sensor response depends on the combustion source and condition. Further information on the
208 combustion sources used in the chamber tests is provided in Table S1.

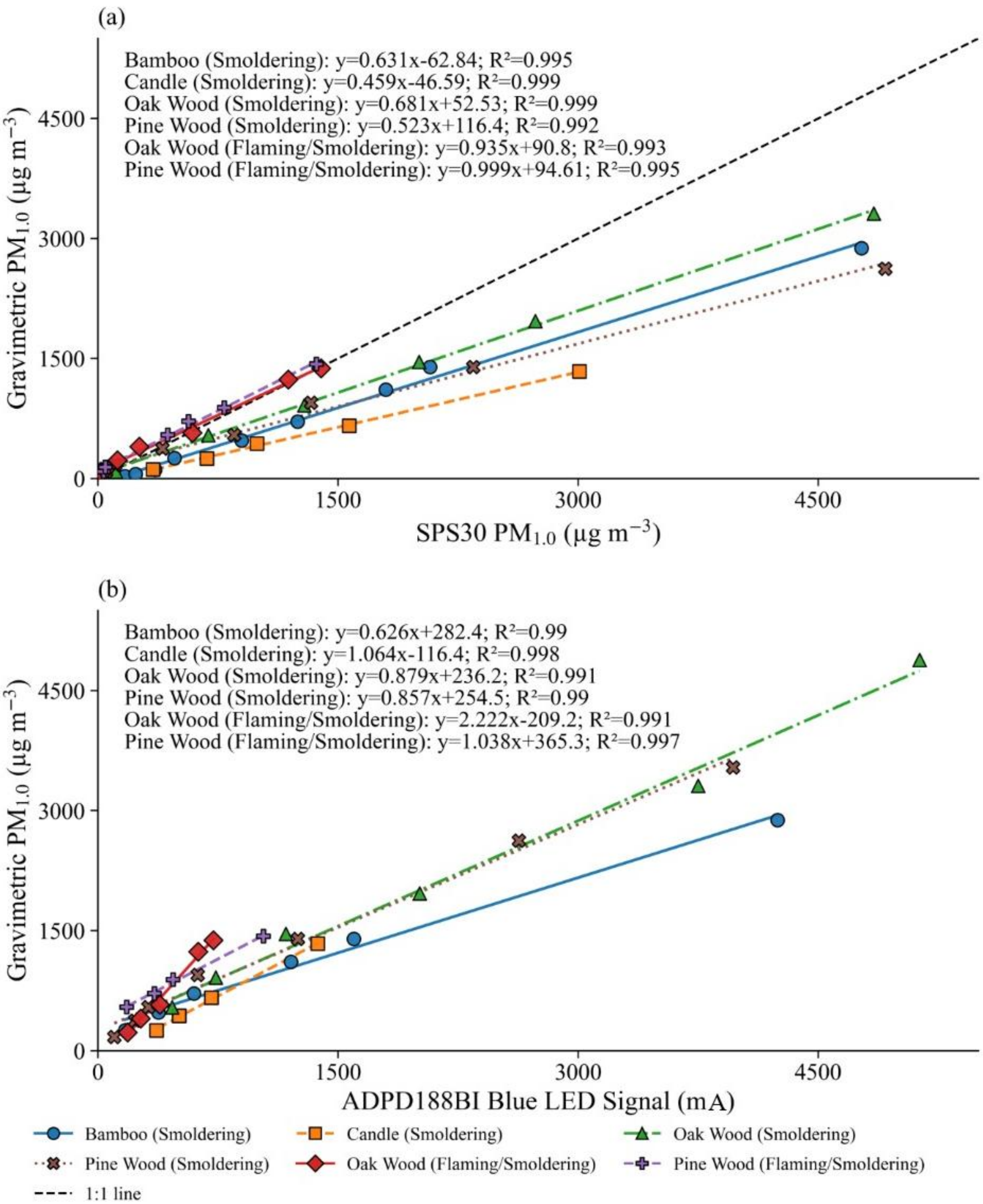

209

https://doi.org/10.5194/egusphere-2026-4763
Preprint. Discussion started: 15 September 2026

Figure 4. Linear relationships between gravimetric $PM_{1.0}$ and (a) SPS30 mass concentration $PM_{1.0}$ and (b) ADPD188BI blue-LED channel signal for candle, bamboo, oak, and pine combustion under either smoldering or smoldering and flaming conditions.

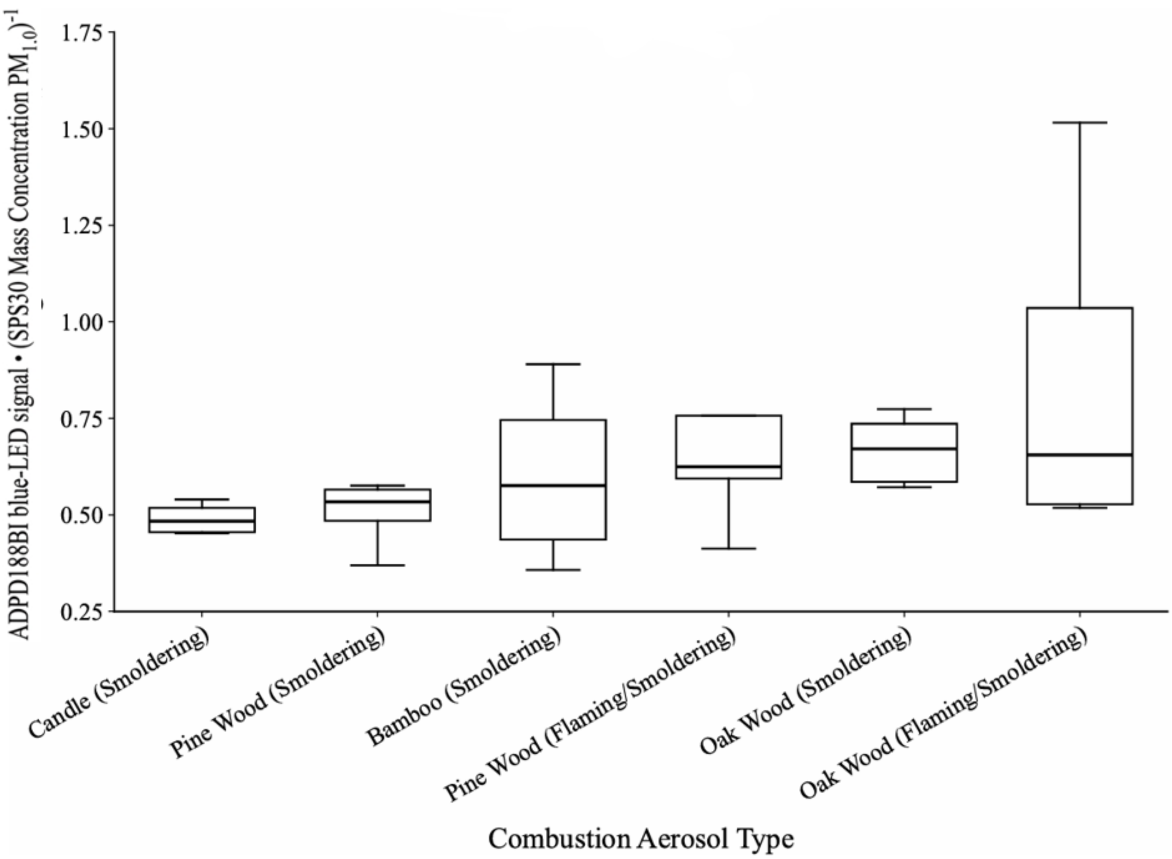

Figure 5. Variation in the relationship between ADPD188BI blue-LED scattering intensity and SPS30 $PM_{1.0}$ mass concentration across combustion aerosols.

The relationship between the SPS30 and ADPD188BI response varied across combustion aerosols (Fig. 5). Differences in the ratio of the two sensor responses indicate source-dependent variation in bulk particle size distribution, which was supported by different size-resolved Lasair contributions for oak and pine flaming

https://doi.org/10.5194/egusphere-2026-4763
Preprint. Discussion started: 15 September 2026

and smoldering aerosols (Fig. S3). Together, these findings show that chamber sensor response depended on combustion-driven changes in aerosol size distribution and support the need for calibration methods that remain robust across varying burn conditions.

Figure 6 shows a strong linear association between the gravimetric-to-SPS30 mass-response coefficient and the ADPD188BI-to-SPS30 response ratio across the tested combustion conditions. The six source-specific response ratios and corresponding mass-response coefficients were used to develop the linear regression shown in Fig. 6. The resulting relationship had a slope of 1.0215, an intercept of −0.0267, and an R^2 of 0.9469. This relationship was then used to estimate the appropriate mass-conversion coefficient from the paired sensor responses for dynamic calibration.

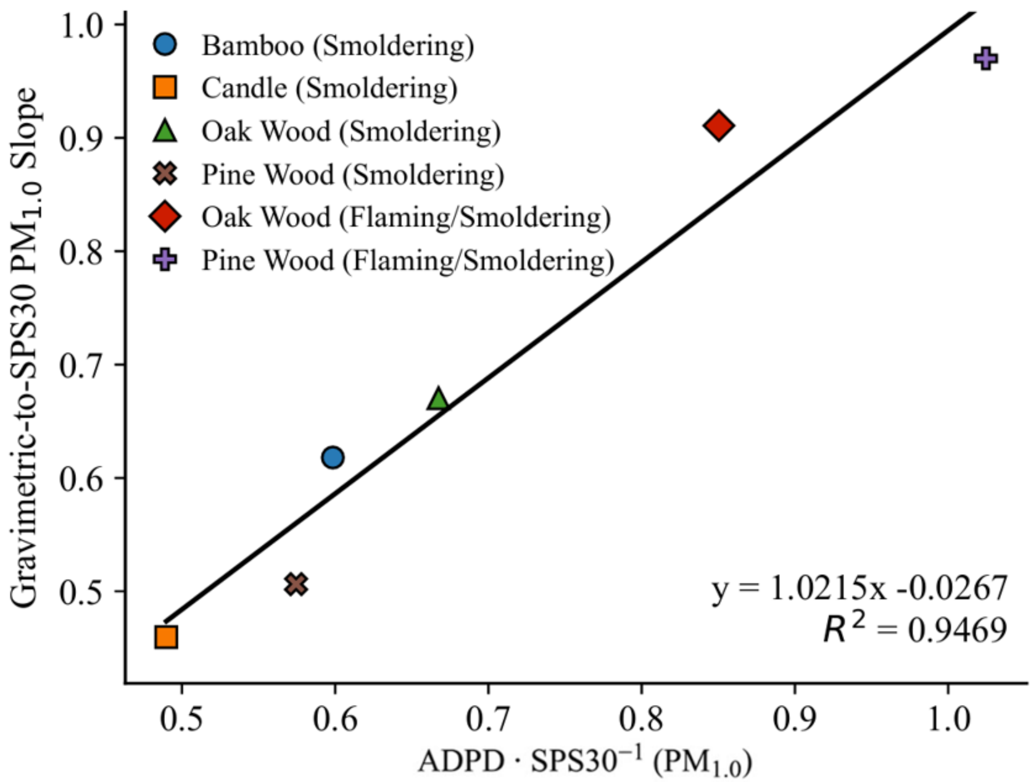

Figure 6. Source-specific relationship between the gravimetric-to-SPS30 mass concentration $PM_{1.0}$ calibration slope and the ADPD188BI blue-LED to SPS30 mass concentration $PM_{1.0}$ response ratio across combustion aerosols.

Rather than requiring prior identification of fuel type or combustion phase, or concurrent measurements with reference instruments, the approach uses the different wavelength dependent sensitivities with particle size of the ADPD188BI and SPS30 to estimate the appropriate mass conversion coefficient in real time,

https://doi.org/10.5194/egusphere-2026-4763
Preprint. Discussion started: 15 September 2026

which would otherwise require source-specific calibration. Figure 7 shows that dynamic calibration improved agreement with gravimetric measurements across all tested combustion aerosol sources, shifting measurements from both smoldering and flaming conditions toward the 1:1 line. The pooled root mean square error (RMSE) decreased from 783.79 to 121.49 µg m^{-3}.

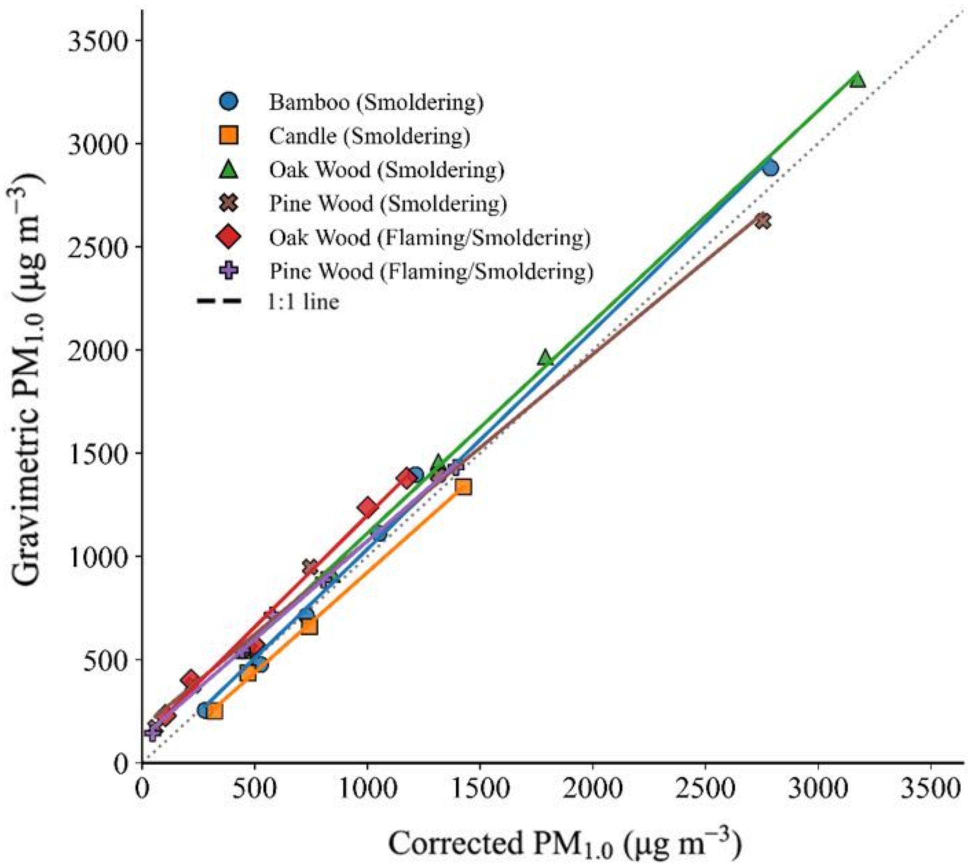

Figure 7. Comparison of dynamically corrected sensor outputs against reference gravimetric $PM_{1.0}$ mass concentrations for various combustion sources. The dotted line represents the 1:1 relationship with gravimetric reference.

https://doi.org/10.5194/egusphere-2026-4763
Preprint. Discussion started: 15 September 2026

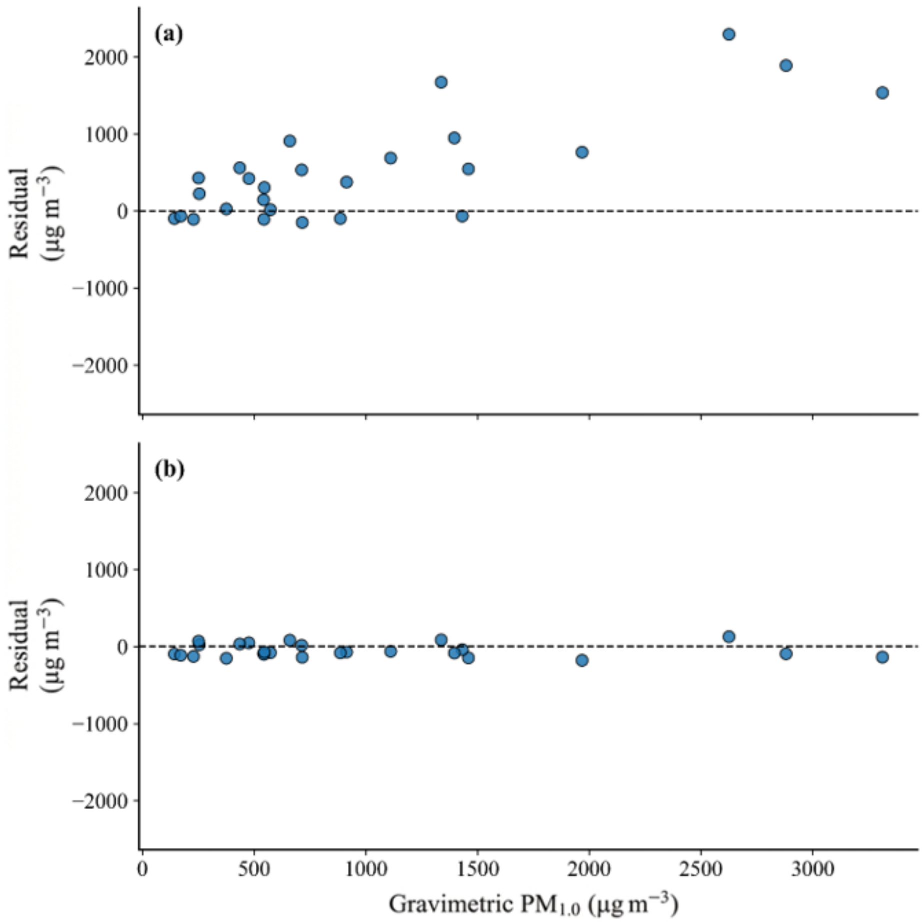

Figure 8. Residual plots for unadjusted and dynamically calibrated SPS30 with combustion aerosols.

Figure 8 presents the residuals for the unadjusted and dynamically calibrated SPS30 measurements relative to gravimetric $PM_{1.0}$. Each blue point represents one paired sensor-gravimetric measurement across the tested combustion conditions. Dynamic calibration reduced the pooled residual RMSE by 84.5 % and centered the residuals more closely around zero.

4 Discussion

Wavelength dependent sensitivities of low-cost particle monitors to particle size result in significant overpredictions and underpredictions in comparison to reference gravimetric mass concentrations with aerosols that have high temporal and spatial heterogeneity, as it cannot account for dynamic changes in particle size distributions (Giordano et al., 2021; Hagan and Kroll, 2020; Tryner et al., 2020). Here we demonstrate that the mass response coefficients for diverse combustion aerosols demonstrated a strong linear association with the ratio of ADPD188BI/SPS30 responses which allows for real time selection of the appropriate mass conversion factors for diverse changing aerosols in a dynamic calibration framework. In practice this enables a dynamic cross-sensor calibration that allows the monitor to adapt in real time to changing combustion sources without prior knowledge of the fuel type. Since fresh biomass-burning aerosol size depends on combustion conditions, with lower combustion efficiencies often producing larger particles, and high-intensity burning tending toward increasing particle size (Reid et al., 2005) , this framework adjusting for bulk particle size differences allows for low-cost sensors to be used as exposure monitors in highly dynamic wildfire environments. The PSL chamber tests confirm the different wavelength dependent sensitivities of the ADPD188BI and SPS30 and the ability to capture a meaningful difference in particle-size-dependent scattering response.

While this calibration adjusts for differences in scattering intensity associated with dynamic changes in the particle size distribution for particles ≥ 0.3 µm, other factors also influence optical mass determination. Multi-factor calibration strategies have been developed for ambient particle monitoring environments that include systematic adjustment for humidity differences (Di Antonio et al., 2018; Zou et al., 2021) and frequently reference to fixed site monitors as a basis for adjustment using data-driven calibration models (Giordano et al., 2021; Kelly et al., 2017; Molina Rueda et al., 2023; Nowack et al., 2021; Tryner et al., 2020; Zou et al., 2021; Zusman et al., 2020). Standard relative-humidity corrections can be incorporated into the dynamic calibration using onboard temperature and relative-humidity measurements. Because reference monitoring sites are often far from active wildfires, direct comparison with reference instruments may not be practical. The proposed approach therefore provides an alternative for field-based smoke monitoring.

The present dynamic calibration approach is limited to the overlapping range of the two sensors, however improvement of the short-wavelength optical designs and lower-noise electronics would likely improve low-end precision and reduce temperature-related variability, to expand sensitivity ranges and make this dynamic calibration approach more widely applicable for ambient and satellite AOD comparisons. Similarly for larger concentrations ranges above 3.4 mg m^{-3} additional sensors in addition to the SPS30 would expand dynamic calibration ranges. While the present system does not explicitly address mass contributions from coarse ash particles, and although Aerodynamic Particle Sizer (APS) measurements indicate that the proportion of particles larger than 1 µm in diameter from smoldering and flaming combustion is very low, coarse material may still be important in some wildfire or mixed-source environments (Dong et al., 2023). The framework could also be evaluated for larger particles using the

https://doi.org/10.5194/egusphere-2026-4763
Preprint. Discussion started: 15 September 2026

SPS30 $PM_{2.5}$, PM_4, and PM_{10}, outputs together with parallel ADPD188BI measurements, although additional testing would be required. Similarly, the range of aerosols tested is limited compared to the wide heterogeneity of aerosols during fires at the wildland urban interface, and with large coarse dust episodes and validation is required to evaluate accuracy of these coefficients under these conditions.

In occupational environments, use of low-cost particle monitors have significant potential and dynamic calibration approaches may address accuracy in relation to reference instruments and the dependency on the type of workplace and how the sensors are used. Overall, these results support the use of paired low-cost optical sensors with different scattering sensitivities as a pathway toward dynamic real-time adjustment of mass response factors for heterogeneous combustion aerosols.

5 Conclusion

Mass-response coefficients across diverse combustion aerosols were strongly associated with the ADPD188BI/SPS30 response ratio, enabling real-time selection of aerosol-specific mass-conversion factors within a dynamic calibration framework. Further validation is needed for the broader aerosol heterogeneity encountered at the wildland–urban interface, including mixed smoke and coarse-dust episodes.

Data Availability

The data underlying the analyses and figures presented in this study are provided in the Supplement.

Supplement Link

The link to the supplement will be included by Copernicus, if applicable.

Author Information

RE conceptualized the study, acquired funding, and supervised the project. RE, MAM, and TA contributed to project administration. MAM curated the data, performed the formal analysis, carried out the investigation, prepared the visualizations, and wrote the original draft. RE and MAM contributed to the methodology and validation. RE and TA provided resources. MAM and TA contributed to software development. RE, MAM, and TA reviewed and edited the manuscript.

Competing Interests

The authors declare that they have no conflict of interest.

Disclaimer

Copernicus Publications remains neutral with regard to jurisdictional claims made in the text, published maps, institutional affiliations, or any other geographical representation in this paper. While Copernicus Publications makes every effort to include appropriate place names, the final responsibility lies with the authors. Views expressed in the text are those of the authors and do not necessarily reflect the views of the publisher.

References

Analog Devices: Integrated Optical Module for Smoke Detection, 2020.

Di Antonio, A., Popoola, O. A. M., Ouyang, B., Saffell, J., and Jones, R. L.: Developing a Relative Humidity Correction for Low-Cost Sensors Measuring Ambient Particulate Matter, Sensors, 18, 2790, https://doi.org/10.3390/s18092790, 2018.

Dong, W.-H., Sheng, X.-E., Wang, S., and Deng, T.: Experimental Study on Particle Size Distribution Characteristics of Aerosol for Fire Detection, Applied Sciences, 13, https://doi.org/10.3390/app13095592, 2023.

Edwards, R., Johnson, M., Dunn, K. H., and Naeher, L. P.: Application of Real-time Particle Sensors to Help Mitigate Exposures of Wildland Firefighters, Arch. Environ. Occup. Health, 60, 40–43, https://doi.org/10.3200/AEOH.60.1.40-43, 2005.

Giordano, M. R., Malings, C., Pandis, S. N., Presto, A. A., McNeill, V. F., Westervelt, D. M., Beekmann, M., and Subramanian, R.: From low-cost sensors to high-quality data: A summary of challenges and best practices for effectively calibrating low-cost particulate matter mass sensors, J. Aerosol Sci., 158, 105833, https://doi.org/10.1016/J.JAEROSCI.2021.105833, 2021.

Hagan, D. H. and Kroll, J. H.: Assessing the accuracy of low-cost optical particle sensors using a physics-based approach, Atmos. Meas. Tech., 13, 6343–6355, https://doi.org/10.5194/amt-13-6343-2020, 2020.

Hinds William and Zhu Yifang: Aerosol_Technology, Third., John Wiley & Sons, Inc., 305–329 pp., 2022.

Jayaratne, R., Liu, X., Ahn, K. H., Asumadu-Sakyi, A., Fisher, G., Gao, J., Mabon, A., Mazaheri, M., Mullins, B., Nyaku, M., Ristovski, Z., Scorgie, Y., Thai, P., Dunbabin, M., and Morawska, L.: Low-cost PM2.5 sensors: An assessment of their suitability for various applications, Aerosol Air Qual. Res., 20, 520–532, https://doi.org/10.4209/aaqr.2018.10.0390, 2020.

Kelly, K. E., Whitaker, J., Petty, A., Widmer, C., Dybwad, A., Sleeth, D., Martin, R., and Butterfield, A.: Ambient and laboratory evaluation of a low-cost particulate matter sensor, Environmental Pollution, 221, 491–500, https://doi.org/10.1016/J.ENVPOL.2016.12.039, 2017.

Khan, M., Khan, N., Skibniewski, M., and Park, C.: Environmental Particulate Matter (PM) Exposure Assessment of Construction Activities Using Low-Cost PM Sensor and Latin Hypercubic Technique, Sustainability, 13, 7797, https://doi.org/10.3390/su13147797, 2021.

https://doi.org/10.5194/egusphere-2026-4763
Preprint. Discussion started: 15 September 2026

Kuula, J., Mäkelä, T., Aurela, M., Teinilä, K., Varjonen, S., González, Ó., and Timonen, H.: Laboratory evaluation of particle-size selectivity of optical low-cost particulate matter sensors, Atmos. Meas. Tech., 13, 2413, 2020.

Molina Rueda, E., Carter, E., L'Orange, C., Quinn, C., and Volckens, J.: Size-Resolved Field Performance of Low-Cost Sensors for Particulate Matter Air Pollution, Environ. Sci. Technol. Lett., 10, 247–253, https://doi.org/10.1021/acs.estlett.3c00030, 2023.

Murphy, G., Bushey, B., and Collins, T.: Passing UL 217 8th Edition: Smoke Detector Reference Design and Algorithm, https://www.scribd.com/document/604282294/AnalogWorld-webinar-presentation-Smoke-Detector, October 2020.

Nowack, P., Konstantinovskiy, L., Gardiner, H., and Cant, J.: Machine Learning Calibration of Low-Cost NO2 and PM10 Sensors: Non-Linear Algorithms and Their Impact on Site Transferability, Atmos. Meas. Tech., 14, 5637–5655, https://doi.org/10.5194/amt-14-5637-2021, 2021.

Penchala, A., Patra, A. K., Mishra, N., and Santra, S.: Field calibration and performance evaluation of low-cost sensors for monitoring airborne PM in the occupational mining environment, J. Aerosol Sci., 184, 106519, https://doi.org/10.1016/J.JAEROSCI.2024.106519, 2025.

Pillarisetti, A., Alnes, L. W. H., Ye, W., McCracken, J. P., Canuz, E., and Smith, K. R.: Repeated assessment of PM2.5 in Guatemalan kitchens cooking with wood: Implications for measurement strategies, Atmos. Environ., 295, 119533, https://doi.org/10.1016/j.atmosenv.2022.119533, 2023.

Reid, J. S., Koppmann, R., Eck, T. F., and Eleuterio, D. P.: A review of biomass burning emissions part II: intensive physical properties of biomass burning particles, Atmos. Chem. Phys., 5, 799–825, https://doi.org/10.5194/acp-5-799-2005, 2005.

Ruiter, S., Kuijpers, E., Saunders, J., Snawder, J., Warren, N., Gorce, J.-P., Blom, M., Krone, T., Bard, D., Pronk, A., and Cauda, E.: Exploring Evaluation Variables for Low-Cost Particulate Matter Monitors to Assess Occupational Exposure, Int. J. Environ. Res. Public Health, 17, https://doi.org/10.3390/ijerph17228602, 2020.

Ruiter, S., Bard, D., Ben Jeddi, H., Saunders, J., Snawder, J., Warren, N., Gorce, J.-P., Cauda, E., Kuijpers, E., and Pronk, A.: Exposure Monitoring Strategies for Applying Low-Cost PM Sensors to Assess Flour Dust in Industrial Bakeries, Ann. Work Expo. Health, 67, 379–391, https://doi.org/10.1093/annweh/wxac088, 2023.

Datasheet SPS30 Particulate Matter Sensor for Air Quality Monitoring and Control:

Tryner, J., Mehaffy, J., Miller-Lionberg, D., and Volckens, J.: Effects of aerosol type and simulated aging on performance of low-cost PM sensors, J. Aerosol Sci., 150, 105654, https://doi.org/10.1016/J.JAEROSCI.2020.105654, 2020.

U.S. Department of Agriculture Forest Service: Appendix A-Smoke From Forest Fires, https://www.fs.usda.gov/t-d/pubs/htmlpubs/htm02252810/page19.htm, 15 October 2016.

U.S. Environmental Protection Agency: Wildfire Smoke - A Complex Mixture.

https://doi.org/10.5194/egusphere-2026-4763
Preprint. Discussion started: 15 September 2026

Zou, Y., Clark, J. D., and May, A. A.: A systematic investigation on the effects of temperature and relative humidity on the performance of eight low-cost particle sensors and devices, J. Aerosol Sci., 152, 105715, https://doi.org/10.1016/J.JAEROSCI.2020.105715, 2021.

Zusman, M., Schumacher, C. S., Gassett, A. J., Spalt, E. W., Austin, E., Larson, T. V, Carvlin, G., Seto, E., Kaufman, J. D., and Sheppard, L.: Calibration of Low-Cost Particulate Matter Sensors: Model Development for a Multi-City Epidemiological Study, Environ. Int., 134, 105329, https://doi.org/10.1016/j.envint.2019.105329, 2020.